VIII SIMPÓSIO DE ESPECIALISTAS EM PLANEJAMENTO DA OPERAÇÃO E EXPANSÃO ELÉTRICA

VIII SYMPOSIUM OF SPECIALISTS IN ELECTRIC OPERATIONAL AND EXPANSION PLANNING

VIII SEPOPE
19 a 23 de Maio de 2002
May - 19th to 23th - 2002
BRASÍLIA (DF) - BRASIL

TWO POWERFUL NETWORK MODELING APPROACHES FOR THE MODAL ANALYSIS OF HARMONIC PROBLEMS

Sergio L. Varricchio, CEPEL
Sergio Gomes Jr., CEPEL
Nelson Martins*, CEPEL
Franklin Clement Véliz, FCTJF

Summary

This paper describes two network modeling approaches. The s-domain or **Y**(*s*) and descriptor system approaches. Both approaches are suitable for perform the modal analysis of the electrical system. Modal analysis provides important system dynamic information that can be used to improve its harmonic performance. The practical use of this dynamic information is shown through the analysis and solution of an industrial system harmonic problem.

Keywords: Network analysis, modal analysis, power system harmonics, poles and zeros, sensitivities.

1. Introduction

Conventional harmonic analysis of electrical systems is based on the computation of the nodal admittance matrix for discrete values of frequency over a desired frequency range. The main advantage of this method is that the admittance matrix is quite straightforward to build. This approach consists basically on frequency response analysis.

On the other hand, modal analysis consists of the calculations of the system poles and transfer function zeros as well as their sensitivities to changes in system parameters. The importance of the modal analysis in the study of harmonic problems has been increasingly emphasized in the technical literature [1]-[5]. It is based on the fact that the harmonic voltage performance of a system depends on the location in the complex plane of its poles and zeros with respect to the critical harmonic frequencies.

The conventional harmonic analysis is performed over the $j\omega$ axis of the complex plane. Thus, only the combined effect of the poles and zeros can be observed from a frequency response of a system transfer function. This analysis does not allow the modal decomposition of the system that is very useful to understand the causes and find cost-effective measures to mitigate harmonic problems.

Some recent papers use the descriptor system approach [3], [4] to model the electrical network for modal analysis. This method automatically deals with state variable redundancies and can be easily and efficiently applied to large-scale networks of any topology. As main drawbacks, this method presents difficulties in modeling frequency dependent parameters and leads to system matrices much larger than the number of system buses.

Another recently proposed method is based on the system nodal admittance matrix in the s-domain, **Y**(*s*) [5]-[8] and also has the ability to compute poles, zeros and residues as well as their sensitivities. Since the electrical network equations are written directly in the complex frequency domain, the modeling of frequency dependent parameters are easily accomplished and the dimension of the **Y**(*s*) matrix is obviously equal to the number of system buses. The main drawback of this method is the impossibility of calculating all system poles at once. The system poles calculation is carried out using Newton based one-eigenvalue-at-a-time iterative methods [6].

This paper will describe some basic ideas behind these two approaches and their use in the study of an industrial system.

2. Network Modeling Approaches

For sake of brevity only the modeling of *RLC* elements will be utilized to present the two approaches. Modeling of transmission lines and two and three-winding power transformers are presented in [9], [10] for descriptor system and in [5], [7] for the s-domain approach.

3. Descriptor System Approach

The dynamic behavior of an electrical network is governed by: Kirchhoff's current law (KCL), Kirchhoff's voltage law (KVL) and the equations describing the inherent dynamic characteristics of each network element [11].

* CEPEL - Caixa Postal 68.007 - CEP 21994-970 - Rio de Janeiro - RJ - Brazil (nelson@cepel.br)

The Kirchhoff's laws (KCL and KVL) are algebraic equations containing the information on system topology. Each algebraic equation determines a linear dependence among system variables (voltages and currents). The dynamic characteristics of the inductive and capacitive elements are described by first order differential equations, in terms of currents and voltages. The inductive currents and capacitive voltages represent the obvious choice of state variables.

The network modeling by the descriptor system technique assumes that all inductive currents and all capacitive voltages are state variables. The interconnection among the various network elements is modeled by a set of equations describing the KCL applied to each system node.

3.1 *RLC Series Branch*

A *RLC* series branch connected between the nodes (buses) *k* and *j* is depicted in Figure 1.

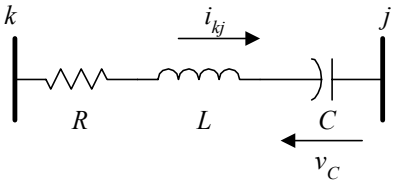

Figure 1: RLC series branch

The electrical behavior of this element can be described by a set of two ordinary differential equations of first order:

$$v_k - v_j = R\, i_{kj} + L\frac{di_{kj}}{dt} + v_C \tag{1}$$

$$C\frac{dv_C}{dt} = i_{kj} \tag{2}$$

where v_k and v_j are the voltages of nodes *k* and *j*, respectively, i_{kj} is the branch current and v_C is the capacitor voltage. When there is no capacitor in the branch, (1) and (2) must be replaced by:

$$R\, i_{kj} + L\frac{di_{kj}}{dt} = v_k - v_j \tag{3}$$

3.2 *RLC Parallel Branch*

A *RLC* parallel branch connected between the nodes *k* and *j* is shown in Figure 2.

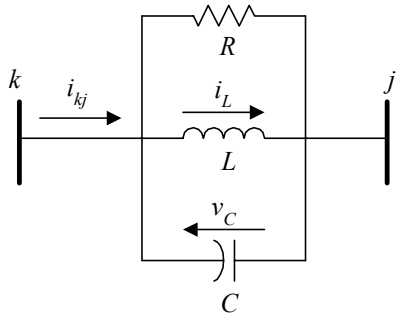

Figure 2: RLC parallel branch

The equations related to this element are:

$$\frac{v_C}{R} + i_L + C\frac{dv_C}{dt} = i_{kj} \tag{4}$$

$$L\frac{di_L}{dt} = v_C \tag{5}$$

$$v_C = v_k - v_j \tag{6}$$

where v_k and v_j are the voltages of nodes *k* and *j*, respectively, i_{kj} is the branch current, v_C is the capacitor voltage and i_L is the inductive current. When there is no inductor in the branch, (4) and (5) must be replaced by:

$$\frac{v_C}{R} + C\frac{dv_C}{dt} = i_{kj} \tag{7}$$

3.3 *KCL Equations*

The KCL equation applied to nodes *k* and *j* (independently of which element are connected between them) yields, respectively:

$$\sum_{m\in\Omega_{(k\neq j)}} i_{mk} - i_{kj} = 0 \tag{8}$$

$$\sum_{m\in\Omega_{(j\neq k)}} i_{mj} + i_{kj} = 0 \tag{9}$$

where $\Omega_{(k\neq j)}$ is the set of all nodes connected to node *k*, except node *j*, similarly $\Omega_{(j\neq k)}$ is the set of all nodes connected to node *j* except node *k*.

Note that i_{kj} in (8) and (9) is a current from node *k* to node *j*, i.e., a positive current injection at *j* and negative at *k*.

After interconnecting the equations for all *RLC* branches, the following descriptor system equation is obtained:

$$\left[\begin{array}{c|c}\mathbf{T}_1 & \mathbf{0} \\ \hline \mathbf{0}^T & \mathbf{0}_q\end{array}\right]\left[\begin{array}{c}\dot{\mathbf{x}}_1 \\ \hline \dot{\mathbf{v}}_{nodal}\end{array}\right]=\left[\begin{array}{c|c}\mathbf{A}_1 & \mathbf{A}_2 \\ \hline \mathbf{A}_3 & \mathbf{0}_q\end{array}\right]\left[\begin{array}{c}\mathbf{x}_1 \\ \hline \mathbf{v}_{nodal}\end{array}\right]+\left[\begin{array}{c}\mathbf{0} \\ \hline \mathbf{I}\end{array}\right]\mathbf{i}_{nodal} \quad (10)$$

$$\mathbf{v}_{nodal}=\left[\mathbf{0}^T \mid \mathbf{I}\right]\left[\begin{array}{c}\mathbf{x}_1 \\ \hline \mathbf{v}_{nodal}\end{array}\right] \quad (11)$$

$\mathbf{T}_1$ is a diagonal matrix and $\mathbf{A}_1$ block-diagonal; $\mathbf{A}_2$ and $\mathbf{A}_3$ are "incidence matrices" for the descriptor system. Symbols $\mathbf{0}$ and $\mathbf{0}_q$ denote null matrices and $\mathbf{I}$ is the identity matrix. The superscript ^{T} denotes matrix transposition and a dot over a vector its time derivative.

The matrix equations (10) and (11) can be written in compact form:

$$\mathbf{T}\,\dot{\mathbf{x}}=\mathbf{A}\,\mathbf{x}+\mathbf{B}\,\mathbf{u} \quad (12)$$

$$\mathbf{y}=\mathbf{C}\,\mathbf{x} \quad (13)$$

where:

$$\mathbf{T}=\left[\begin{array}{c|c}\mathbf{T}_1 & \mathbf{0} \\ \hline \mathbf{0}^T & \mathbf{0}_q\end{array}\right] \qquad \mathbf{A}=\left[\begin{array}{c|c}\mathbf{A}_1 & \mathbf{A}_2 \\ \hline \mathbf{A}_3 & \mathbf{0}_q\end{array}\right]$$

$$\mathbf{B}=\left[\begin{array}{c}\mathbf{0} \\ \hline \mathbf{I}\end{array}\right] \qquad \mathbf{C}=\left[\mathbf{0}^T \mid \mathbf{I}\right]$$

$$\mathbf{u}=\mathbf{i}_{nodal} \qquad \mathbf{y}=\mathbf{v}_{nodal}$$

4. S-Domain Approach

The network is modeled by the $\mathbf{Y}(s)$ matrix, where s is the complex frequency given by $s=\sigma+j\omega$. This matrix is built just as the nodal admittance matrix $\mathbf{Y}(j\omega)$. Thus, a diagonal element y_{ii} of the nodal matrix $\mathbf{Y}(s)$ is calculated as the summation of all elementary admittances connected to node i. On the other hand, the off-diagonal elements y_{ij} are equal to the negative value of the summation of all elementary admittances connected between the nodes i and j.

Replacing the purely imaginary frequency $j\omega$ for the complex frequency s is needed to perform modal analysis.

The first derivative of $\mathbf{Y}(s)$ with respect to the complex frequency s is also required [5] - [7] for use in the Newton eigensolution algorithms. This derivative can be easily obtained following similar rules to those for building the $\mathbf{Y}(s)$ matrix. For instance, consider a parallel and a series RLC branch. They have the following admittances as complex frequency functions:

$$y_{parallel}=\frac{1}{R}+\frac{1}{sL}+sC \quad (14)$$

$$y_{series}=\frac{sC}{s^2LC+sRC+1} \quad (15)$$

The derivatives with respect to s of (14) and (15) are given, respectively, by:

$$\frac{dy_{parallel}}{ds}=C-\frac{1}{s^2L} \quad (16)$$

$$\frac{dy_{series}}{ds}=-\frac{\left(s^2LC-1\right)}{Cs^2}y_{series}^2 \quad (17)$$

5. The Industrial System

The harmonic problem investigated in this paper is related to the industrial system shown in Figure 3. The data related to the linear loads, capacitor banks, transformers and bus voltage are shown in this figure. The linear loads were modeled by parallel RL branches. The 138 kV system is modeled as a voltage source in series with an equivalent short circuit impedance. All the circuits (lines) in the industrial system studied have the same electric parameters per-unit length (equal to $R=0.133\ \Omega/\text{km}$, $\omega L=0.39\ \Omega/\text{km}$ and $C=0.0132\ \mu F/\text{km}$) and were modeled using single π-circuits. The line lengths (in km) are given in Table 4.

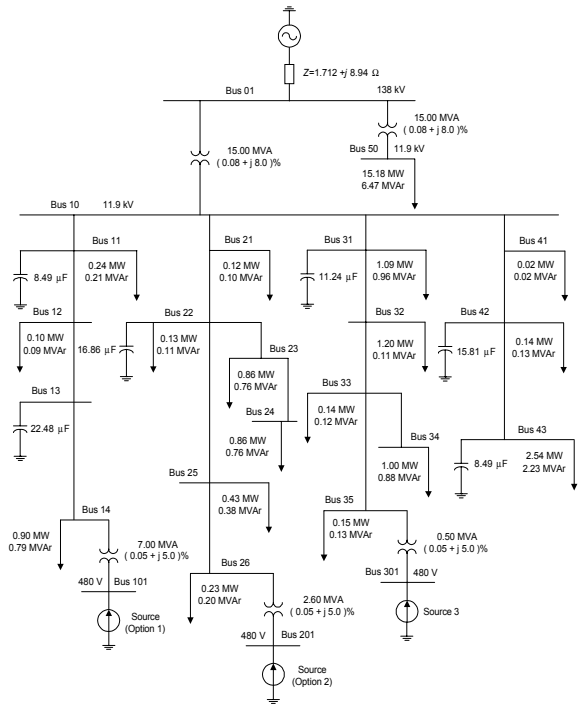

Figure 3: Industrial system

Table 1: Line lengths of the industrial system

Bus from	Bus to	length	Bus from	Bus to	length
10	11	1.4	25	26	1.0
11	12	0.9	10	31	1.1
12	13	0.8	31	32	0.7
13	14	0.7	32	33	1.3
10	21	1.0	33	34	1.2
21	22	0.9	33	35	0.7
22	23	1.2	10	41	0.8
22	25	0.8	41	42	0.8
23	24	1.5	42	43	1.3

The harmonic problem consists in choosing, between buses 101 (option 1) or 201 (option 2), which is the best bus for placing a 12-pulse industrial rectifier. The total current at fundamental frequency drawn by this rectifier is 5.5 kA. The harmonic current components (I_h) are given in Table 2 as percentage values of its fundamental current.

Table 2: Harmonic current components

h	11	13	23	25
I_h(%)	9.0	8.0	4.0	4.0

6. Analysis of Option 1

The modulus of the transfer-impedance between the buses 101 and 13 ($Z_{101,13}$) is plotted in Figure 4. The bus 13 was chosen in this tutorial example for having high harmonic distortions.

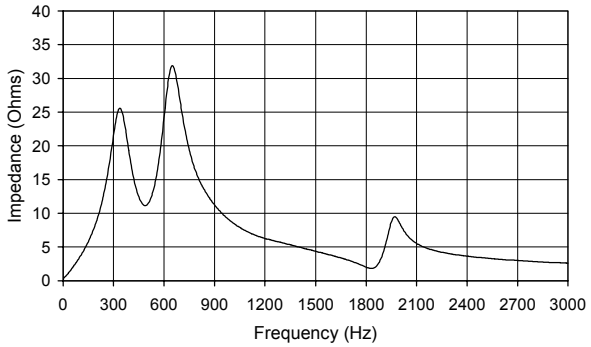

Figure 4: Transfer-impedance $Z_{101,13}$

The industrial system was modeled by the two described approaches. The system poles and transfer functions (transfer impedances) zeros can be calculated using Newton based one-eigenvalue-at-a-time iterative methods [6] using either one of the two methods. For the descriptor system there is also the option of calculating all eigenvalues at once using the **QZ** eigenroutine [12]. In this case the poles are the generalized eigenvalues of finite modulus of the matrix pair $\{\mathbf{A}, \mathbf{T}\}$. Both modeling approaches yield exactly the same results.

It must be pointed out that if one wants to model some set of frequency dependent parameter this could be accomplished very easily by using the s-domain approach. In this case this set could be, firstly, fixed at its fundamental frequency values and the descriptor system approach could be used to calculate all poles and zeros at once using the QZ eigenroutine. The numerical values of these poles and zeros could then be used as initial guess for a Newton based one-eigenvalue-at-a-time iterative methods using the s-domain approach and taking into account the frequency variation of the parameter set.

The imaginary parts of the poles divided by 2π are the parallel frequency resonance or the frequencies (in Hz) associated with the poles. Similarly the imaginary parts of the zeros divided by 2π are the series frequency resonance or the frequencies associated with the zeros. The frequencies associated with the poles and their sensitivities [1] - [5] to the capacitances of the industrial system are presented in Table 3. These sensitivities are given in Hz/μF. Similarly, the frequencies associated with the zeros of the transfer-impedance $Z_{101,13}$ and their sensitivities are given in Table 4. In these tables C_{13} denotes the capacitor connected at bus 13 and so on.

The poles of the industrial system and $Z_{101,13}$ zeros spectra are shown in Figure 5. Note that only those poles and zeros with frequencies in the range between zero and 1500 Hz were plotted in this figure.

Table 3: Frequency associated with the poles and their sensitivities to capacitor changes

	P_1	P_2	P_3	P_4	P_5	P_6
f(Hz)→	337	640	829	1233	1916	1959
C_{11}	-1.936	-0.903	0.004	-0.697	0.836	-99.888
C_{13}	-2.731	-7.048	-0.242	-0.541	-0.170	-3.978
C_{22}	-1.682	-1.635	-16.108	-3.294	-0.124	-0.083
C_{31}	-1.387	-0.571	-0.527	-46.357	-1.701	-2.152
C_{42}	-1.815	-3.978	-3.890	-0.286	-25.237	-3.511
C_{43}	-2.036	-6.260	-8.375	-2.971	-63.705	5.768

Table 4: Frequency associated with the zeros of $Z_{101,13}$ and their sensitivities to cap. changes

	Z_1	Z_2	Z_3	Z_4	Z_5
f(Hz)→	495	825	1221	1849	1938
C_{11}	-0.659	-0.109	-1.981	-99.619	-3.721
C_{13}	0.000	0.000	0.000	0.000	0.000
C_{22}	-4.121	-14.941	-3.814	-0.242	0.004
C_{31}	-2.588	-0.550	-44.867	-5.162	0.200
C_{42}	-5.207	-4.578	-0.344	0.918	-29.679
C_{43}	-6.786	-9.716	-3.307	-4.331	-53.585

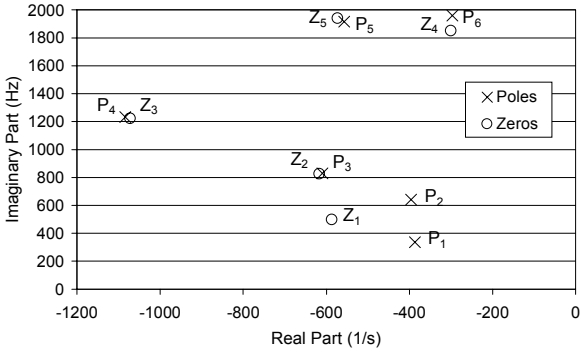

Figure 5: Poles of the industrial system and $Z_{101,13}$ zeros spectra

It is worth noting that the shapes of the impedance plot, (Bode diagram) shown in Figure 4, may be sketched by hand from the inspection of the associated pole-zero spectra. One can observe, for instance, that the poles P_3, P_4 and P_5 are very close to the zeros Z_2, Z_3 and Z_5, respectively. This proximity cancels the effect of these

poles and zeros in the impedance plot. Actually, to obtain this canceling effect, it would only be necessary to have closer frequencies associated with these poles and zeros (imaginary parts).

As one can see from Figure 4 and Figure 5 the pole located at 640 Hz (pole P_2) is the most responsible for possible high distortions mainly at 11º and 13º harmonic frequencies (660 Hz and 780 Hz, respectively). From Table 3 it is possible to see that this pole has the highest sensitivity with respect to changes in the capacitor C_{13}. On the other hand from Table 4 it is possible to see that the zero located at 495 Hz (zero Z_1) has null sensitivity to this capacitor. This means that if this capacitor is increased the frequency associated with P_2 will decrease (negative sensitivity) and may become closer to zero Z_1, being therefore partially canceled. In terms of the Bode diagram shown in Figure 4 the second peak will be shifted to the left and its amplitude will diminish. In fact the first peak will also be shifted to the left since the pole P_1 has a negative sensitivity to this capacitor. The poles of the industrial system and $Z_{101,13}$ zeros spectra and the impedance plot diagram for $C_{13} = 42.48\,\mu F$ (which means an additional capacitance of $\Delta C_{13} = 20.0\,\mu F$) are shown in Figure 6 and Figure 7, respectively. The original plots are superimposed for easy comparison.

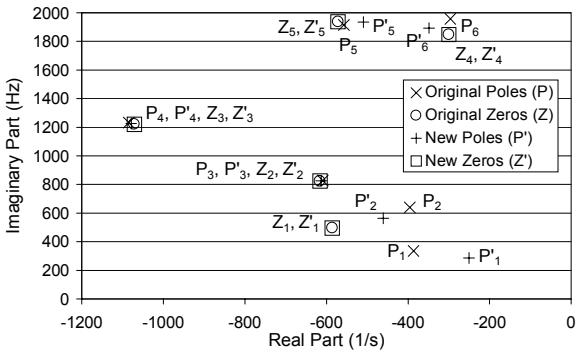

Figure 6: Poles of the industrial system and $Z_{101,13}$ zeros spectra for $C_{13} = 42.48\,\mu F$

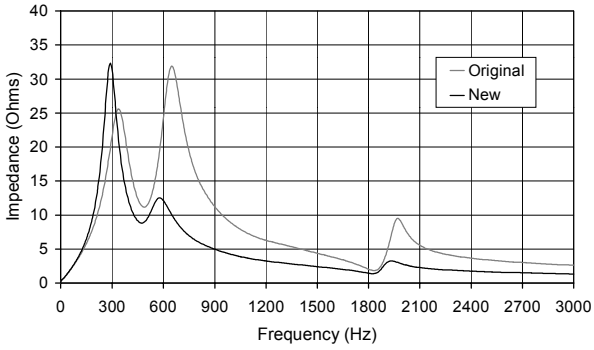

Figure 7: Transfer-impedance $Z_{101,13}$ for $C_{13} = 42.48\,\mu F$

The new values of the frequencies associated with the system poles are presented in Table 5 for $C_{13} = 42.48\,\mu F$. Since the sensitivities of the frequencies associated with the $Z_{101,13}$ zeros with respect to changes in the capacitance C_{13} are all nulls (see second row of Table 4) their values and their sensitivities remain the same.

Table 5: Frequency associated with the system poles for $C_{13} = 42.48\,\mu F$

	P_1	P_2	P_3	P_4	P_5	P_6
f(Hz)→	288	564	827	1227	1895	1936

The voltage distortions for the original system and for the proposed solution are listed in Table 6 as well as the distortion limits [13] adopted in this paper. The voltage distortions that exceed the maximum accepted limits are highlighted.

Table 6: Harmonic voltage distortion spectrum at bus 13

Harmonic Order	Original System (%)	Proposed Solution (%)	Limits (%)
11	9.15	2.78	3.5
13	4.33	1.65	3.0
23	0.662	0.350	1.5
25	0.563	0.309	1.5

7. Analysis of Option 2

The modulus of the transfer-impedance between the buses 201 and 22 ($Z_{201,22}$) is plotted in. The bus 22 was chosen for the same reasons as before (see Section 6).

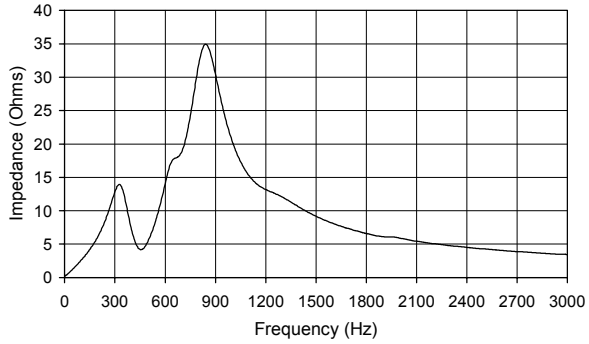

Figure 8: Transfer-impedance $Z_{201,22}$

The frequencies associated with the zeros of the transfer-impedance $Z_{201,22}$ and their sensitivities are given in Table 7. The poles and their sensitivities do not depend on the transfer function considered, being already presented in Table 3. The poles of the industrial system and $Z_{201,22}$ zeros spectra is shown in Figure 9.

Table 7: Frequency associated with the zeros of $Z_{201,22}$ and their sensitivities to cap. changes

	Z_1	Z_2	Z_3	Z_4	Z_5
f(Hz)→	450	670	1199	1914	1958
C_{11}	-3.018	-0.269	-0.900	-0.700	-98.199
C_{13}	-6.258	-3.683	-0.798	-0.257	-3.908
C_{22}	0.000	0.000	0.000	0.000	0.000
C_{31}	-1.063	-0.735	-47.545	-1.959	-2.180
C_{42}	-1.892	-7.970	-0.552	-24.396	-4.303
C_{43}	-2.227	-13.092	-4.552	-63.444	5.446

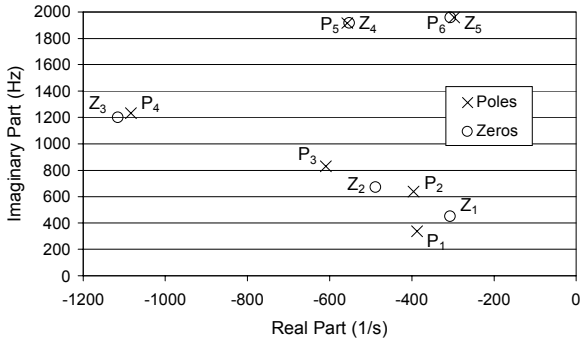

Figure 9: Poles of the industrial system and $Z_{201,22}$ zeros spectra

As one can see from Figure 8 and Figure 9, the pole located at 829 Hz (pole P_3) contributes for possible high distortions mainly at 11^{o} and 13^{o} harmonic frequencies (660 Hz and 780 Hz, respectively). From Table 3 it is possible to see that this pole has the highest sensitivity to the capacitor C_{22}. On the other hand from Table 7 it is possible to see that the zero located at 670 Hz (zero Z_2) has null sensitivity to this capacitor. This means that if this capacitor is increased the frequency associated with P_3 will decrease (negative sensitivity) and will become closer to zero Z_2, being therefore partially canceled. On the other hand the pole P_2, which is partially canceled by the zero Z_2, will move away from Z_2 and its effect will become more evident. Note in the Bode diagram of Figure 8 that the peak associated with pole P_3 will be shifted to the left and its amplitude will be reduced. Also the peak associated with pole P_2 will be shifted to the left but its amplitude will increase. The poles of the industrial system and $Z_{201,22}$ zeros spectra and the impedance plot diagram for $C_{22} = 26.86\,\mu F$ (which mean an additional capacitance of $\Delta C_{22} = 10.0\,\mu F$) are shown in Figure 10 and Figure 11, respectively. The original plots are superimposed for easy comparison.

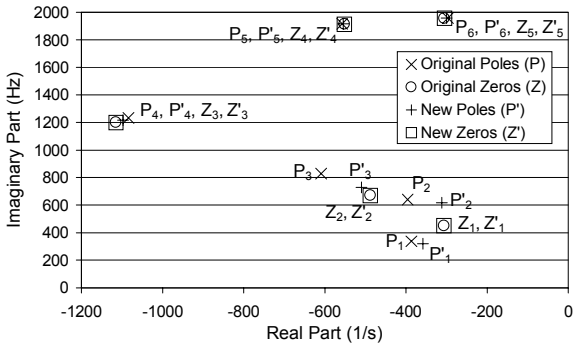

Figure 10: Poles of the industrial system and $Z_{201,22}$ zeros spectra for $C_{22} = 26.86\,\mu F$

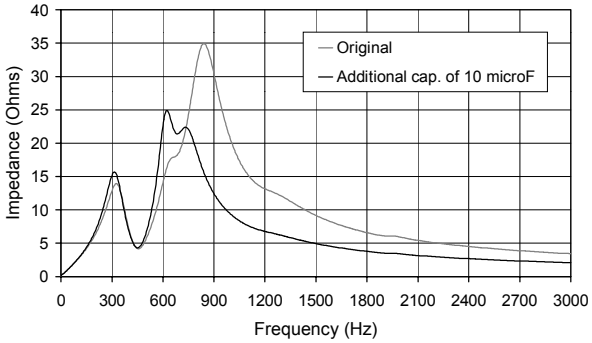

Figure 11: Transfer-impedance $Z_{201,22}$ for $C_{22} = 26.86\,\mu F$

The new values of the frequencies associated with the industrial system poles are presented in Table 8 for $C_{22} = 26.86\,\mu F$. Since the sensitivities of the frequencies associated with the $Z_{201,22}$ zeros to the capacitance C_{22} are all nulls (see second row of Table 7) their values and their sensitivities remain unaltered.

Table 8: Frequency associated with the poles and their sensitivities to cap. changes for $C_{22} = 26.86\,\mu F$

	P_1	P_2	P_3	P_4	P_5	P_6
f(Hz)→	321	616	729	1216	1915	1958
C_{11}	-1.591	-1.284	-0.007	-0.808	0.312	-99.316
C_{13}	-2.175	-7.587	-0.151	-0.668	-0.201	-3.955
C_{22}	-1.677	-3.275	-5.358	-0.845	-0.044	-0.024
C_{31}	-1.185	-0.240	-0.060	-47.422	-1.799	-2.172
C_{42}	-1.505	-1.213	-6.941	-0.406	-24.920	-3.808
C_{43}	-1.669	-1.789	-12.465	-3.737	-63.681	5.715

From Table 8 and Figure 10 it is possible to see that if the capacitor C_{22} is increased again, the pole P_3 can be totally canceled by the zero Z_2. Note from Table 7 that the sensitivity of Z_2 to C_{22} is null, thus it will stay still. For similar reasoning its possible to conclude that the pole P_2 will become closer to zero Z_1, being partially canceled. In terms of Bode diagram show in Figure 11 the peak associated with pole P_3 will vanish and the peak associated with pole P_2 will be shifted to the left

and its amplitude will be reduced. The impedance Bode diagram for $C_{22} = 46.86\,\mu F$ (which means an additional capacitance of $\Delta C_{22} = 30.0\,\mu F$) is shown in Figure 12. The original plots are superimposed for easy comparison.

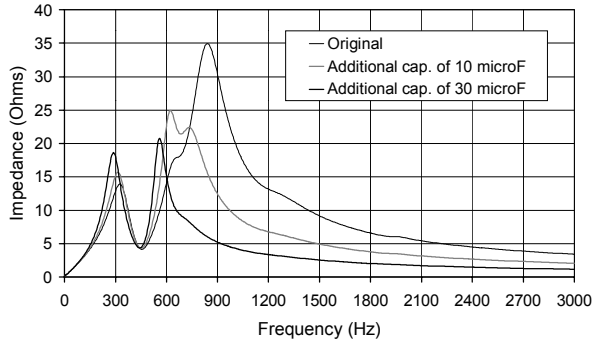

Figure 12: Transfer-impedance $Z_{201,22}$ for $C_{22} = 46.86\,\mu F$

The voltage distortions for the original system and for the proposed solution are listed in Table 9.

Table 9: Harmonic voltage distortion spectrum at bus 22

Harmonic Order	Original System (%)	Proposed Solution (%)	Limits (%)
11	5.20	2.89	3.5
13	7.48	1.85	3.0
23	1.40	0.368	1.5
25	1.18	0.330	1.5

In Figure 13 the final transfer-impedances $Z_{101,13}$ and $Z_{201,22}$ are plotted together to show the equivalence of the two solutions. The Option 1 is preferred since it requires 10.0 μF less than the Option 2.

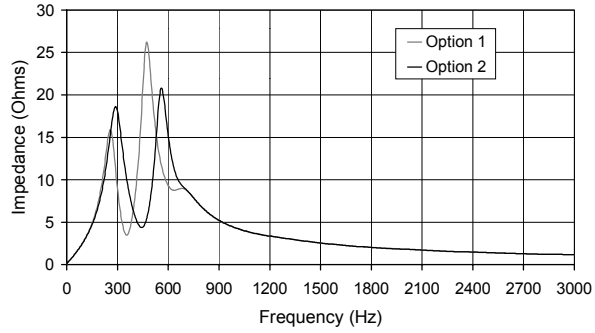

Figure 13: Final transfer-impedances $Z_{101,13}$ and $Z_{201,22}$

8. Remarks

For Option 2 it is interesting to see what is the effect of connecting the additional capacitance of 30μF at bus 26 (the closest 11.9 kV bus of the non-linear load) instead of bus 22. The transfer impedances $Z_{201,22}$ for both cases are shown in Figure 14. The distortions at bus 22 for the additional capacitance at bus 26 are listed in Table 10.

As one can see the additional capacitance connected at bus 22 has reduced the distortions at high harmonic frequency, acting therefore as a high-pass filter. On the other hand, when connected at bus 26, has amplified them. This simple example shows the importance of investing on the development of methodologies to effectively determine the optimum placing of new equipment.

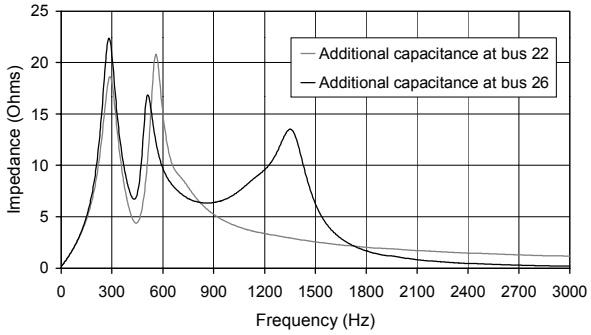

Figure 14: Transfer-impedances $Z_{201,22}$ for additional capacitance at bus 22 and bus 26

Table 10: Harmonic voltage distortion spectrum at bus 22 for additional capacitance at bus 26

Harmonic Order	Original System (%)	Proposed Solution (%)	Limits (%)
11	5.20	2.33	3.5
13	7.48	1.69	3.0
23	1.40	1.67	1.5
25	1.18	0.808	1.5

9. Conclusions

Some basic ideas about two network modeling approaches were presented in this paper. The $\mathbf{Y}(s)$ approach is considered to be a natural evolution of the conventional $\mathbf{Y}(j\omega)$ approach. The $\mathbf{Y}(s)$ approach allows obtaining all the results that can be obtained by the $\mathbf{Y}(j\omega)$ approach. Additionally, the $\mathbf{Y}(s)$ approach allows modal analysis to be performed. The descriptor system approach can be used as a powerful complement of the $\mathbf{Y}(s)$ approach since it allows the computation of the complete set of system poles and transfer function zeros at once.

The modal analysis gives important system dynamic information that can be used to improve the harmonic performance of a system. This was shown through the simple example presented in this paper.

The practical use of modal analysis in power quality problems is still in its infancy. Further work will try using this technology to the optimum design of passive filters.

10. Bibliography

[1] Thomas H. Ortmeyer and Khaled Zehar, "Distribution System Harmonic Design", *IEEE Transaction on Power Delivery*, Vol. 6, No. 1, January 1991.

[2] J. Martinon, P. Fauquembergue and J. Lachaume, "A State Variable Approach to Harmonic Disturbances in Distribution Networks", *7th International Conference on Harmonics and Quality of Power - 7th ICHQP*, Las Vegas, USA, 16th - 18th October, 1996, pp. 293-299.

[3] S. L. Varricchio, N. Martins, L. T. G. Lima and S. Carneiro Jr. "Studying Harmonic Problems Using a Descriptor System Approach", *Proceedings of the IPST'99 - International Conference on Power System Transients*, Budapest, Hungary, June, 1999.

[4] Sergio L. Varricchio and Nelson Martins, "Filter Design Using a Newton-Raphson Method Based on Eigenvalue Sensitivity", *IEEE Proceedings of the Summer Power Meeting*, July 16-20, 2000, Seattle, Washington, USA.

[5] Sergio L. Varricchio, Sergio Gomes Jr., Nelson Martins "S-Domain Approach to Reduce Harmonic Voltage Distortions Using Sensitivity Analysis", *IEEE Proceedings of the Winter Power Meeting*, Columbus, Ohio, USA, 28 January – 1 February, 2000.

[6] Sergio Gomes Jr., Nelson Martins and Carlos Portela "Modal Analysis Applied to s-Domain Models of ac Networks", *IEEE PES Winter Meeting*, Columbus, Ohio, January 2000.

[7] S. Gomes Jr., C. Portela, N. Martins, "Detailed Model of Long Transmission Lines for Modal Analysis of ac Networks", *Proceedings of the IPST'01 - International Conference on Power System Transients*, Rio de Janeiro, Brazil, June 2001.

[8] A. Semlyen, "s-Domain Methodology for Assessing the Small Signal Stability of Complex Systems in Non-Sinusoidal Steady State", *IEEE Transactions on Power Systems*, vol. 6, no. 1, February 1999, pp. 132-137.

[9] Leonardo T. G. Lima, Nelson Martins and Sandoval Carneiro Jr., "Dynamic Equivalents for Electromagnetic Transient Analysis Including Frequency-Dependent Transmission Line Parameters", Proceedings of the IPST'97 International Power System Transients Conference, Seattle, USA, July, 1997.

[10] Leonardo T. G. Lima, "Applications of Descriptor System to Electromagnetic Transient Analysis of Large Scale Networks" (in Portuguese), Ph.D. Thesis, COPPE/UFRJ, Rio de Janeiro, Brazil, 1999.

[11] L. O. Chua and P. M. Lin, "Computer-Aided Analysis of Electronic Circuits: Algorithms and Computational Techniques", Prentice-Hall, Inc., Englewood Cliffs, NJ, USA, 1975.

[12] G. H. Golub and C. F. Van Loan, "Matrix Computations", The Johns Hopkins University Press, 1989.

[13] IEC 1000-3-6-Electromagnetic Compatibility (EMC), Part 3, Section 6: "Assessment of Emission Limits for Distortion Loads in MV and HV Power Systems", First Edition, 1996-10.